Corrosion Fatigue Crack Growth in 7050 Aluminum Alloy Extrusions

J.M. Van Orden* and D.E. Pettit*
Lockheed-California Company, Burbank, Calif.

As part of a continuing program to provide data to aid in the prediction of materials' behavior, tests were conducted to compare the effects of various corrosive environments on the fatigue crack propagation rates of several 7075-T76511 and 7050-T76511 extruded shapes. The ASTM E399 compact specimen was used, and test variables included stress intensity (ΔK) and grain direction, with the stress range ratio and test frequency being held constant ($R=0.1$, 6 Hz). Other tests included static mechanical properties, constant amplitude fatigue, fracture toughness, stress corrosion resistance, and exfoliation corrosion resistance. The tests showed that the fatigue strengths of the two alloys were similar except that, in the low-load, high-cycle range, the 7050-T76511 provided a slight advantage. Fracture toughness (K_{Ic}) ranged from 17 to 50 ksi$\sqrt{\text{in.}}$ and was found to vary significantly with specimen orientation. Fatigue crack growth rates (DA/DN) in the various test environment increased in the following order: dry air, moist air, sump water, salt water. The effect of test environment was more prominent than specimen orientation at $\Delta K < 0.8\,(1-R)(K_{Ic})$. As ΔK approached $(1-R)(K_{Ic})$, however, the effect of large differences in K_{Ic} (with specimen orientation) increased. Fatigue crack growth rates were comparable for the two alloys in salt water, but, in dry air, rates were slightly higher for 7075-T76511. The results of the tests generally showed that higher fracture toughness did not improve resistance to fatigue crack growth; however, higher-toughness material did tolerate more stable crack growth before failure and, therefore, would provide improved tolerance to crack damage, i.e., longer life, in a service environment.

I. Introduction

HIGH-STRENGTH aluminum alloys such as 7075-T6 offer design advantages over the lower-strength alloys by permitting reduction in vehicle weight and increases in performance. The advantages due to higher strength, however, are partially offset by poor stress corrosion and exfoliation corrosion resistance. These factors increase the cost of using the higher-strength alloys because of requirements for corrosion protection, more detailed inspection, more frequent maintenance, and possible service failure. The presence of residual tensile stress promotes stress and exfoliation corrosion. Therefore, residual stresses resulting from heat treatment and assembly must be minimized by limiting heat treatment section sizes, degreee of fastener interference fit, and mismatch tolerances. These factors also increase the cost of using these alloys. A partial solution to these problems became available during the 1960's with the development of age-stabilized tempers; for example, 7075-T76 and 7075-T73. The improvements in corrosion resistance, however, were offset by significant reductions in strength, thereby incurring weight penalties.

A more acceptable solution to the problem has been achieved through the recent development of alloys such as 7049, 7050, and 7475. Improvements in stress corrosion and exfoliation corrosion resistance were achieved with little or no loss in tensile strength.[1-7] Before these materials can be considered for structural applications, other design properties must be determined, e.g., fatigue, fracture toughness, and fatigue crack growth in corrosive environments, and the results compared with data derived from materials in current use. Accordingly, Lockheed has been evaluating these materials on a continuing basis, with a major emphasis on the 7050 alloy in the form of extruded shapes. In addition to the standard mechanical properties tests (i.e., tensile, compression, shear, and bearing), tests also were conducted to determine the constant amplitude fatigue properties, fracture toughness, stress corrosion resistance, exfoliation corrosion resistance, and fatigue crack growth rates in corrosive environments. Comparison tests were conducted using the currently used 7075-T76511 alloy. The program was aimed at 1) comparing the performance of the two compositions under identical test conditions, 2) evaluating the variation in properties in the 7050 composition produced by several of the major mill suppliers in the form of several extruded shapes, and 3) providing data for the prediction of the behavior of the 7050 alloy in simulated service environments.

II. Test Materials and Test Specimens

The test materials evaluated in this program included two integrally stiffened aircraft structural wing plank extrusions (codes X and W), a heavy H-shaped keelson extrusion (code Z), and two L-shaped spar extrusions (codes Y and S). The 7050-T76511 extrusions were supplied by three mill suppliers, in the overall cross-sectional dimensions illustrated in Fig. 1. Comparison tests were conducted on the 7075-T6511 (code U) and 7075-T76511 (code V) in the form of wing plank extrusion obtained from production stock. These particular production extrusions had the same shape as the code X extrusions mentioned earlier. The chemical compositions of the materials are given in Table 1. The zinc content of code X material was below the 5.7% minimum for 7050. The only apparent effects were slightly lower tensile and compression strengths. Other properties were comparable with the other 7050 extrusions.

Presented as Paper 75-806 at the AIAA/ASME/SAE 16th Structures, Structural Dynamics, and Materials Conference, Denver, Colo.; May 27-29, 1975; submitted May 27, 1975; revision received March 4, 1976. The authors are indebted to many prople at Lockheed-California Company and several of the major aluminum mill suppliers (Kaiser Aluminum, Martin-Marietta Aluminum, and Aluminum Company of America), and their contributions in the planning, material procurement, testing, and analysis phases are acknowledged gratefully. Special recognition is accorded J.H. Wooley, G.G. Wald, R. Brodie, J. Ekvall, V. Moss, T. Lunde, D. Hoeppner, W. Krupp, S. Krystkowiak, W. Fitze, and L. Barker of Kaiser Aluminum; W. Rotsell and D. Mellem of Martin-Marietta Aluminum; and P. Mehr, A. Kuhns, and H. Larner of Aluminum Company of America, all of whom worked with the authors during the the program.

Index categories: Aircraft Structural Materials; Materials, Properties of.

*Research Scientist, Structures and Materials Laboratory.

Accordingly, the code X material was designated as X7050-T76511.

In addition to standard mechnical property test specimens, fracture toughness, stress corrosion, and fatigue crack growth test specimens were prepared. Fracture toughness and fatigue crack growth specimens were prepared in accordance with the ASTM E399 compact specimen with $B=0.75$ in. $= W/2$ and $W/4$, respectively.

Stress corrosion test specimens were machined as small tensile specimens 1.25 in. long, with a 0.125-in.-diam, 0.5-in.-long test section. Most of the test specimens were machined from the thicker sections of the extruded shapes and from the base of the planks. Mechanical properties and stress corrosion results are presented in Table 2.

III. Testing

Duplicate or triplicate fracture toughness tests were conducted in accordance with the procedures outlined in ASTM E399-72 utilizing the compact specimen with $B=0.75$ in. $=0.5W$. Triplicate stress corrosion test specimens were loaded axially in test fixtures to three stress levels and exposed to alternate immersion (10 min immersed, 50 min dry per cycle) in a 3.5% sodium chloride-water solution for a period of 30 days and inspected daily for failures. The alternate immersion test procedure is described in MIL-H-6088D. Failure criteria are visual fracture and metallographic examination per ASTM G47-76.

Fatigue crack propagation tests were conducted under plane strain stress intensity conditions on one specimen for each material/test condition. The specimens were fatigue-precracked in air at $R=+0.1$ and 6 Hz to a length of approximately 0.10 in. Decreasing loads were used during precracking so that the final 0.02-in. increment of crack length was generated at a stress intensity equal to the initial test stress intensity. After precracking, the test specimens were heated at 150°F for 10 min before the environmental chamber

Table 1 Chemical compositions of 7075 and 7050 extrusions (two samples)[a]

Material (element)	Code U, V 7075 (1 in. plank)	Code X X7050 (1 in. plank)	Code W 7050 (1 in. plank)	Code Y 7050 (1.4 in. spar)	Code Z 7050 (1.3 in. keelson)	Code S 7050 (1 in. spar)
Silicon	0.120	0.090	0.090	0.085	0.070	0.075
Iron	0.210	0.130	0.095	0.090	0.085	0.085
Copper	1.33	2.36	2.21	2.23	2.21	2.23
Manganese	0.020	0.015	0.010	0.010	0.010	0.010
Magnesium	2.34	2.22	2.35	2.32	2.33	2.31
Chromium	0.250	0.015	0.010	0.010	0.010	0.010
Zinc	5.46	4.94[b]	5.91	5.94	5.91	5.89
Titanium	0.030	0.020	0.045	0.030	0.030	0.020
Zirconium	0.001	0.105	0.095	0.095	0.110	0.105
Aluminum	Rem	Rem	Rem	Rem	Rem	Rem

[a] Code U, V supplied by Production Stock, codes X and Z by Martin-Marietta Aluminum, codes W and Y by Aluminum Company of America, and code S by Kaiser Aluminum.
[b] Below the 5.7% minimum required for 7050; therefore, code X will be indentified as X7050 in this paper.

Table 2 Static mechanical properties of 7075 and 7050 extrusion

Material	Grain direction	F_{tu} ksi	F_{ty} ksi	e %	F_{cy} ksi	F_{su} ksi	F_{bru} ksi, e/D 1.5	F_{bru} ksi, e/D 2.0	K_{Ic}[a] ksi√in.	SCC[b] ksi
7070-T6511	L	92	84	12	72[c]	43[c]	116[c]	145[c]	29(LT)[c]	....
(code U),	LT	85	75	12	72[c]	....	....	....	23(TL)[c]	....
(1 in. plank)	ST	81	70	10	....	....	....	....	20(SL)[c]	<10
7075-T76511[d]	L	82	73	10	65[c]	40[b]	109[c]	138[c]	29(LT)	....
(code V)	LT	77	68	10	65[c]	....	....	....	24(TL)	....
(1 in. plank)	ST	74	65	7	....	....	....	....	19(SL)	>30
X7050-T76511[d]	L	84	76	11	73	....	120	....	30(LT)	....
(code X)	LT	78	71	10	76	42	118	....	24(TL)	....
(1 in. plank)	ST	78	69	5	....	37	....	....	19(SL)	25
7050-T7611[d]	L	87	79	13	78	....	....	....	33(LT)	....
(code W)	LT	81	74	10	79	....	....	....	....	....
(1 in. plank)	ST	78	72	5	....	....	....	....	25(TL) 50(LS)	30
7050-T76511	L	87	79	13	....	....	....	....	32(LT)	....
(code Y)	LT	82	75	13	....	....	....	....	24(TL)	....
(1.4 in. base)	ST	80	73	9	....	....	....	....	27(SL)	>35
7050-T76511	L	88	82	12	78	48	120	157	30(LT)	....
(code Z)	LT	82	75	9	81	46	118	158	19(TL)	....
(1.3 in. cap)	ST	81	71	7	....	....	....	....	17(SL)	35
7050-T76511	L	85	78	14	....	....	....	....	39(LT)	....
(code S)	LT	82	75	12	....	....	....	....	27(TL)	....
(1 in. base)	ST	82	71	10	....	....	....	....	....	25

[a] Letters in parentheses indicate test specimen orientations.
[b] The lowest stress without fracturing in 30 days' alternate immersion in 3.5% NaCl.
[c] MIL-HDBK-5 data; F_{su} and F_{bru} grain direction not specified.
[d] Plank tensile specimens taken near edge; longitudinal center data were 2 ksi lower in codes X and W and 5 ksi lower in code V.

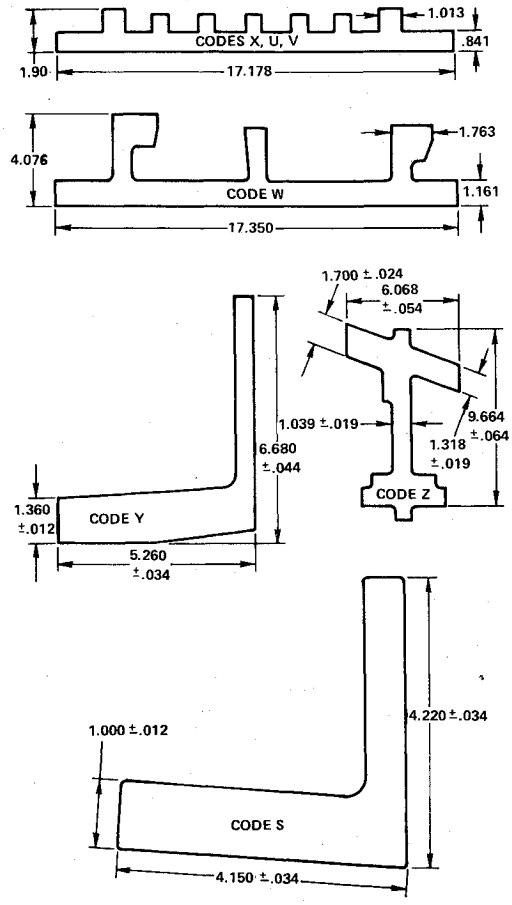

Fig. 1 Extruded shapes used in the test.

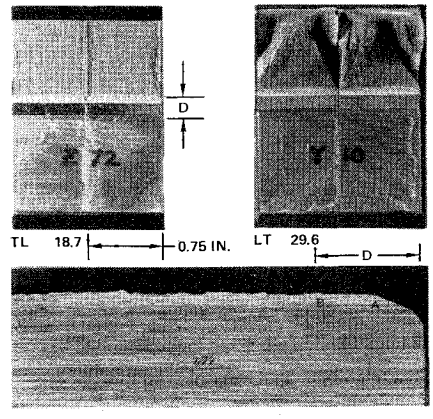

Fig. 2 Fracture surfaces of 7050-T76511 extrusion codes Z and Y specimens illustrating flat and mixed fracture paths (upper photographs) and section through specimen Z72 at 5× showing fracture edge and grain flow (lower photograph). The notch root is at *A*, the fatigue precrack front is at *B*, and the remainder is the fast fracture surface. Test specimen orientations and K_{Ic} values are indicated.

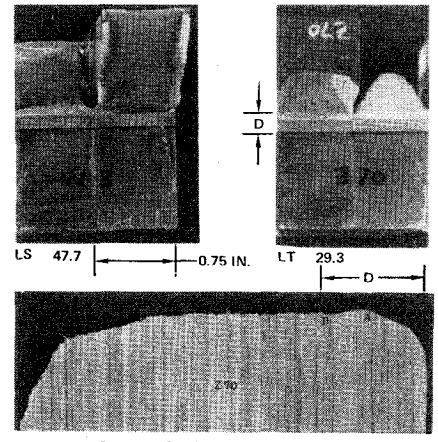

Fig. 3 Fracture surfaces of 7050-T76511 extrusion codes W and Z specimens illustrating 45° and 90° fracture paths (upper photographs) and section through specimen Z70 at 5× showing fracture edge and grain flow (lower photograph). The notch root is at *A*, the fatigue precrack front is at *B*, and the remainder is the fast fracture surface. Test specimen orientations and K_{Ic} values are indicated.

was placed around the specimen. Tests were conducted in dry air [< 8% relative humidity (RH)], moist air (approximately 80% RH), simulated sump tank water,[8] and 3.5% sodium-chloride solution.

Crack-growth tests were conducted beginning with an initial load equal to the final precracking load and then with incrementally increased loads until final fracture. A range ratio of +0.1 and a frequency of 6 Hz were used for the entire test. Crack growth was measured optically and recorded at 0.015-in. to 0.020-in. growth increments. All tests were performed in servo-controlled electrohydraulic fatigue machines with peak and valley load monitoring so that maximum and minimum loads per cycle were controlled within ±1% of maximum load.

The cyclic test load vs crack length data were converted into crack growth rate (DA/DN) vs stress intensity factor (ΔK) according to established practice, using a FORTRAN computer program operating on an XDS Sigma 5 computer. In this program, the stress intensity factor (ΔK value), corresponding to each measured increment of crack growth , is computed on the basis of the average crack length in the interval $(a_i + a_{i+1})/2$, and the varying component of fatigue stress, which is a function of the load and is given by the formula $\Delta P = (1 - R)P$. The formulation for ΔK is otherwise identical to that for K as given in ASTM E399-72. The tests were limited to the range $0.45 \leq a/W \leq 0.7$. The crack growth rate during each increment is approximated by the relation $(a_{i+1} - a_i)/(N_{i+1} - N_i)$. The results, in the form of DA/DN vs ΔK, were plotted automatically using a Calcomp plotter.

A log-log printout format was examined, and the results were found not to conform to a simple power law expression of the form $DA/DN = C\Delta K^n$. Because of the wide variety of nonlinear expressions available in the literature, a simple semilog graphical presentation format was utilized. This format was selected for maximum data resolution.

IV. Results

Fracture Toughness Tests

The fracture toughness test results presented in Table 2 showed significant variations in toughness values with specimen orientation. The values were highest for the *LT* orientation where the 7050-T76511 code S spar showed the highest toughness value, 39 ksi$\sqrt{\text{in.}}$ and the 7075-T6511 and −T76511 showed the lowest value, 29 ksi$\sqrt{\text{in.}}$ In this orientation, *L* is the direction of loading, longitudinal in the extrusion in this case, and *T* is the direction of crack growth, the width direction in this case.

Other orientations showed lower values, with the 7050-T76511 code *Z* extrusion showing the lowest value, 17 ksi $\sqrt{\text{in.}}$ in the *SL* orientation. For the *SL* orientation, the crack growth was parallel to the longitudinal grain direction (*L*), and loading was in the thickness direction (*S*). Typical fracture surfaces for some of these specimens are shown in Figs. 2 and 3 to illustrate the deviation from flat fracture in the *LT*- and *LS*-oriented specimens to a direction parallel with the grain flow. These specimens were loaded in a direction parallel to the grain flow pattern.

In the *TL*-oriented specimens, the entire fracture surface was flat. These were loaded in a direction normal to the grain flow; the plane of the fracture face was parallel to the grain flow. The difference in fracture toughness among the orien-

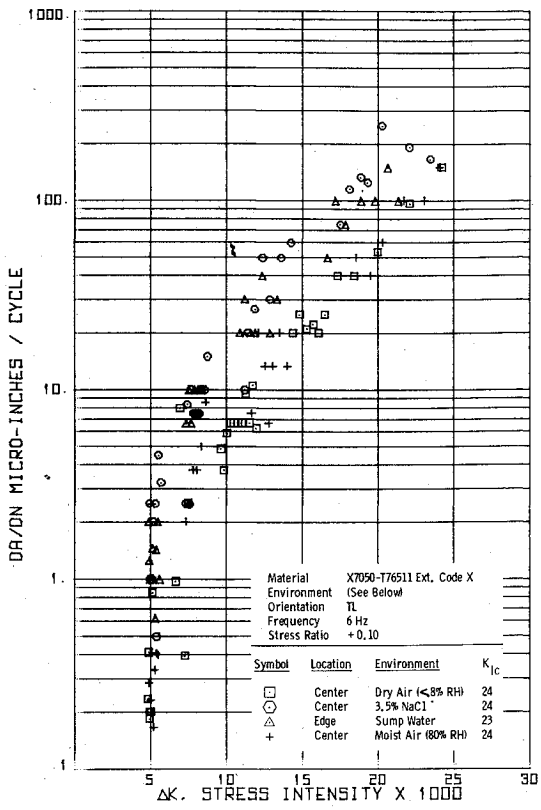

Fig. 4 Effect of environment on X7050-T76511 extrusion.

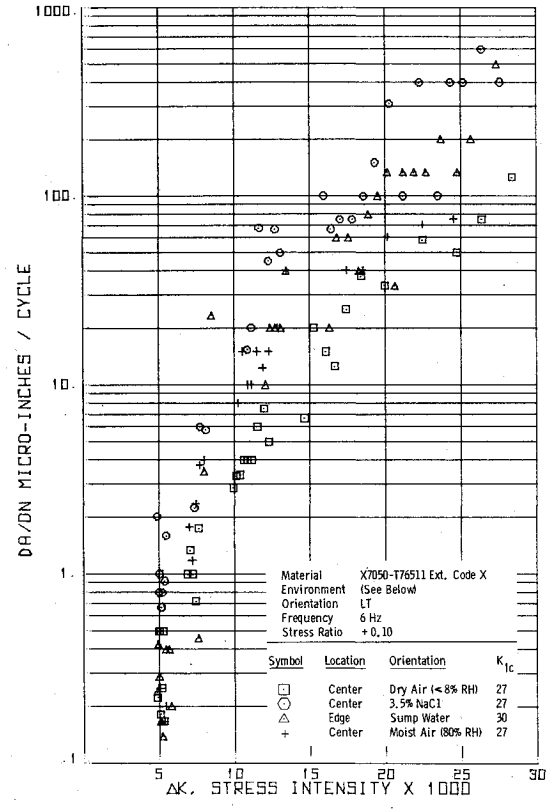

Fig. 5 Effect of environment on X7050-T76511 extrusion.

tations was significant. These fracture path deviations also were observed on the test specimens made from the other extrusions, and similar differences were observed in the fracture toughness test results. In these tests, the advancing crack tends to follow the grain flow during fast fracture.

Stress Corrosion Tests

The results of the stress corrosion tests are presented in Table 2. These data relfect considerable improvement in both the 7075-T76511 and 7050-T76511 over the 7075-T6511 material. The stress corrosion threshold stress for the 7050-T76511 ranged from 25 ksi in the code S extrusion and the code X plank to 30 ksi in the code W extrusion and 35 ksi in the codes Z and Y extrusions. The threshold stress for the 7075-T76511 code V extrusion was greater than 30 ksi (the highest test stress level for this extrusion). The stress corrosion threshold stress for the 7075-T6511 code U extrusion was less than 10 ksi.

Fatigue Crack Growth Tests

The plane-strain fatigue crack growth rate data are plotted in Figs. 4–12. As shown in Figs. 4 and 5, the fatigue crack growth rates for X7050-T76511 extruded plank increased in the various environments in the following order: dry air, moist air, sump water, and salt water. Typical data are shown in Fig. 4 for test specimens in which the crack growth was parallel with the longitudinal grain direction (*TL* orientation). Similar results were obtained with *LT*-oriented specimens, which displayed crack growth rates similar to the *TL*-oriented specimens in all but the dry air environment, where the crack growth rates were lower in the *LT*-oriented specimens. This is illustrated in Fig. 5.

Tests on the effects of test specimen orientation (*LT* and *TL*) and location (edge and center or midwidth) in the plank material showed lower crack growth rates for the *LT*-oriented specimens in both center- and edge-located specimens tested in dry air. Crack growths were comparable in the edge and center locations for each orientation. In salt water, sump water, and moist air, the crack growth rates were not affected significantly by specimen orientation or location at lower ΔK

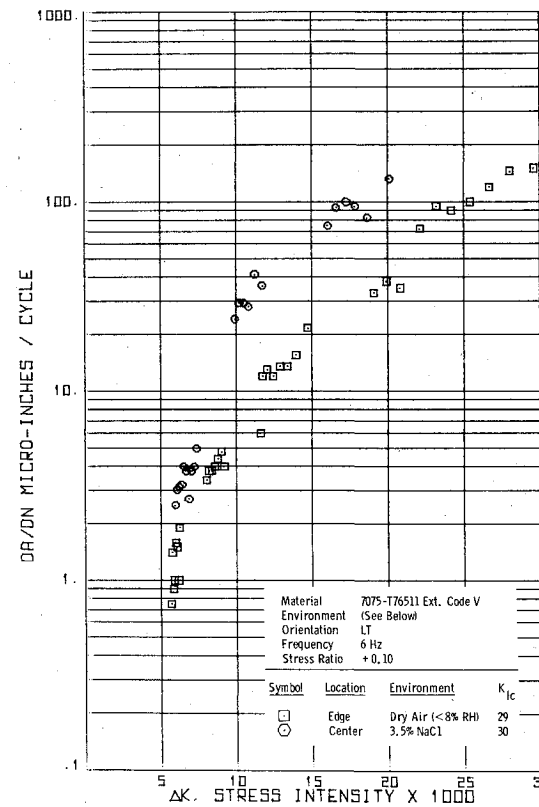

Fig. 6 Effect of environment on 7075-T76511 extrusion.

levels (below 20 ksi$\sqrt{\text{in}}$. At higher ΔK values, in all of the environments, the higher toughness in the *LT* orientation generally permitted stable fatigue crack growth to continue at greater ΔK values (above 20 ksi$\sqrt{\text{in}}$.).

Of all common test environments, dry air is the least aggressive, and salt water is one of the most aggressive.

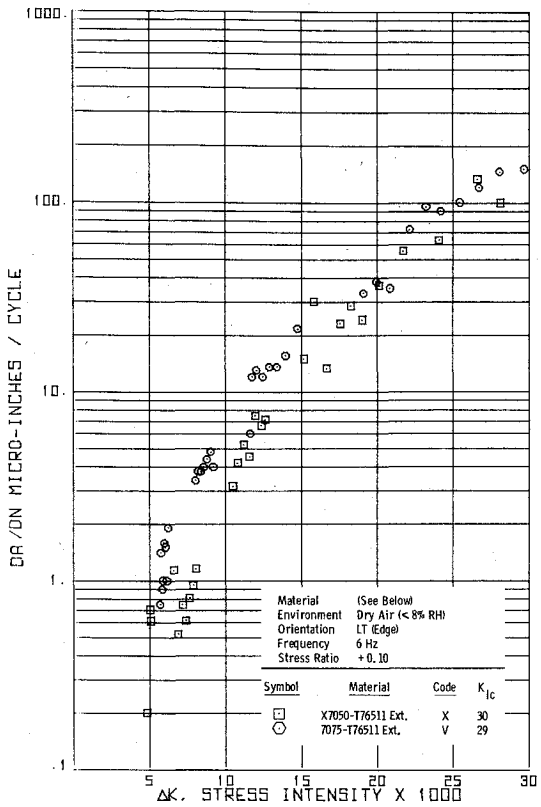

Fig. 7 Comparative crack growth of X7050 and 7075 extrusion in dry air.

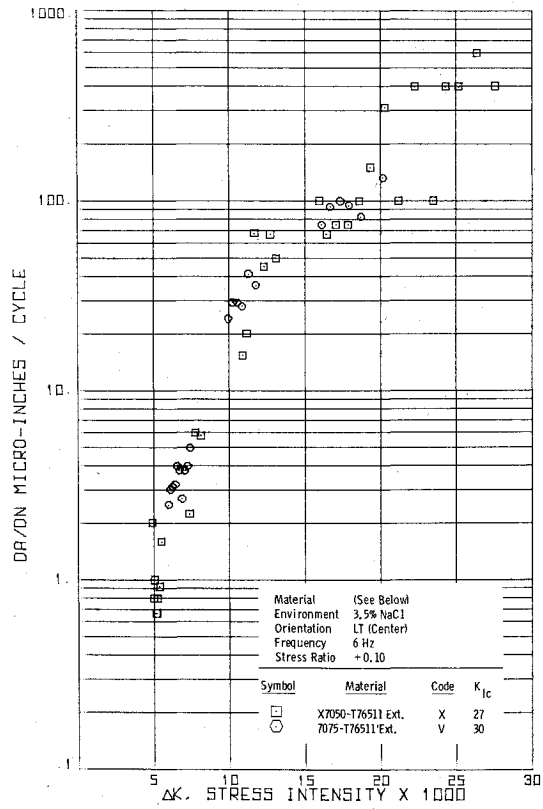

Fig. 8 Comparative crack growth of X7050 and 7075 extrusion in salt water.

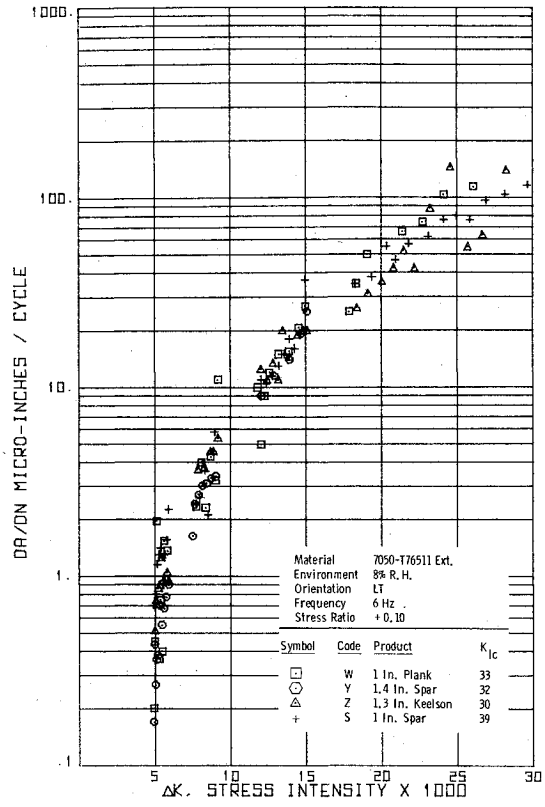

Fig. 9 Crack growth rates for 7050 extrusions in dry air: *LT* orientation.

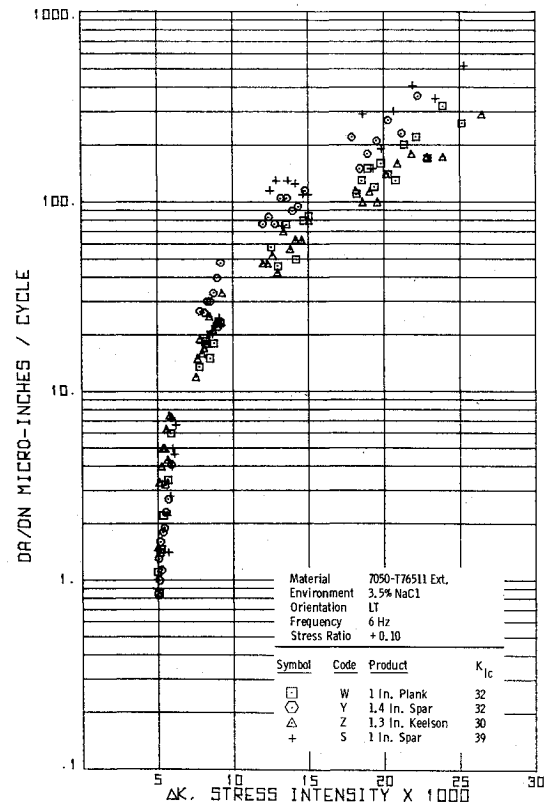

Fig. 10 Crack growth rates for 7050 extrusions in salt water: *LT* orientation.

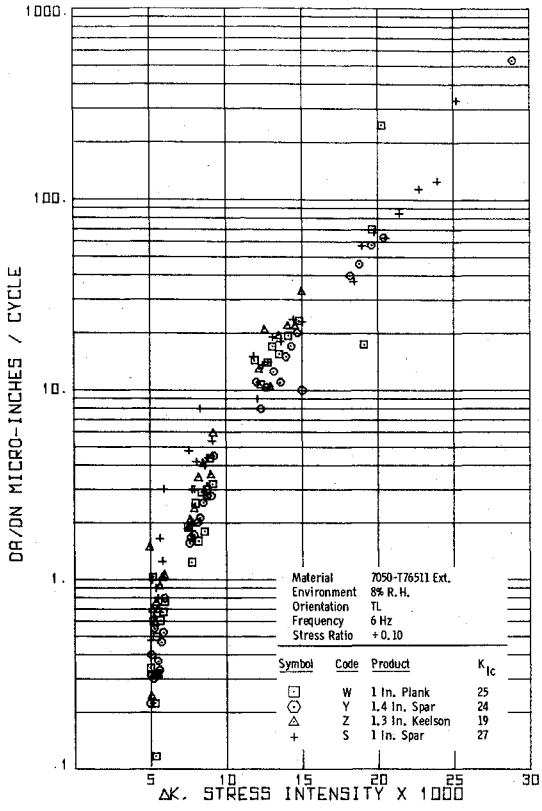

Fig. 11 Crack growth rates for 7050 extrusions in dry air: *TL* orientation.

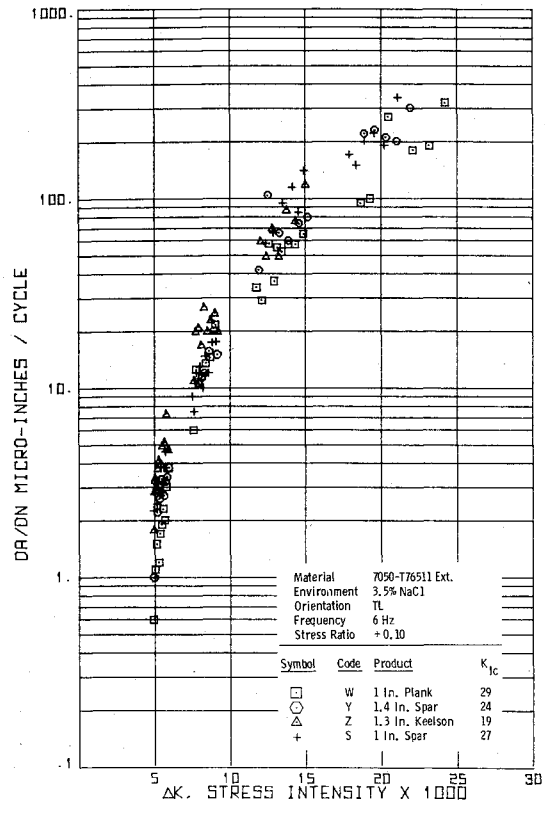

Fig. 12 Crack growth rates for 7050 extrusions in salt water: *TL* orientation.

Therefore, tests were performed on the 7075-T76511 extruded plank in each of these environments to provide comparative data for both of these limiting conditions. The effect of the salt water on crack growth rate of 7075-T76511 is illustrated in Fig. 6. The crack growth rate in dry air was slightly higher for the *TL*-oriented 7075-T76511 specimens than for the *LT*-oriented specimens; whereas, rates in salt water were similar for the two orientations. The higher crack growth rates in salt water also were observed with the X7050-T76511 material (compare Figs. 4 and 6).

Comparative crack growth rates for the two materials are illustrated in Figs. 7 and 8 for dry air and salt water environments. In dry air, the rate was slightly higher at intermediate stress intensities for the 7075-T76511 (Fig. 7). In salt water, however, the rates were comparable for the two materials (Fig. 8), even though the 7075-T76511 failed earlier (at $\Delta K = 20$ ksi$\sqrt{\text{in.}}$) than the X7050-T76511.

Fatigue crack growth data for several additional 7050-T76511 extruded product shapes (i.e., 1-in. plank, 1.4-in. spar, 1.3-in. keelson, and 1-in. spar), which were supplied by three of the major mill suppliers, are compared in Figs. 9-12. The data show significantly higher crack growth rates in the salt water environment but only slight differences among the products within each environment. For example, the crack growth rates in salt water for *LT* specimens were slightly higher for the 1.4- and the 1-in. spars above $\Delta K + 10$ ksi$\sqrt{\text{in.}}$ (Fig. 10). In the *TL* specimens, the rates were comparable in salt water for the four shapes (Fig. 12), although the code Z specimen failed early (at $\Delta K = 15$ ksi$\sqrt{\text{in.}}$).

In the 1-in. plank, the crack growth rates in the *LT* and *TL* orientations were comparable in each of the two test environments, although the rates for both orientations were much higher in salt water, as illustrated in Fig. 5 for X7050-T76511. Similar results were observed for the other three shapes, although in the 1.3-in. keelson, the *TL* specimens failed at a stress intensity of approximately 15 ksi$\sqrt{\text{in.}}$ in both environments. The *LT* specimens, however, survived to stress intensities between 25 and 30 ksi$\sqrt{\text{in.}}$

These test results have demonstrated that fatigue crack growth rates of 7075-T76511 and 7050-T76511 in corrosive environments were comparable in the *TL* and *LT* orientations. This was true even though the fracture toughness values showed a difference of approximately 30% with orientation for the 7050-T76511, and approximately 12% for the 7075-T76511. In the dry air test, the *TL* crack growth rates for the 1-in. spar extrusion (code S) were approximately double those of the *LT* rates at stress intensities above 20 ksi$\sqrt{\text{in.}}$ Moreover, the dry air *TL* rates were approximately twice the *LT* rates in the code X extrusion at stress intensities above 15 ksi$\sqrt{\text{in.}}$ and in the 7075-T76511 extrusion code V at stress intensities aboue 10 ksi$\sqrt{\text{in.}}$ It should be pointed out, however, that these differences between rates in the *LT* and *TL* orientations may not be significant if one considers specimen-to-specimen variations (up to 2.5 times) typically observed in current state-of-the-art testing.[9]

V. Discussion

The results of this program have shown that the tensile strength properties of the 7050-T76511 extrusions are slightly lower than comparable 7075-T6511 properties, but they are significantly higher than 7075-T76511 properties. The code X 7050-T76511 extrusion properties were only slightly higher than those of the 7075-T76511, and it is believed that this may have been due to the low zinc content (1% lower than the other 7050-T76511 extrusions; see Table 1) in this extrusion. Fracture toughness values were generally slightly higher overall in the 7050-T76511 extrusions than the 7075-T76511 extrusions in the *LT* orientation and were more nearly equivalent in the other orientations.

Perhaps the most significant finding revealed by this effort was the apparent lack of significant correlation of plane strain fatigue crack propagation rates in corrosive environments with fracture toughness. The higher fracture toughness values associated with the *LT* specimen orientation generally showed little effect on crack growth rates under the test conditions at

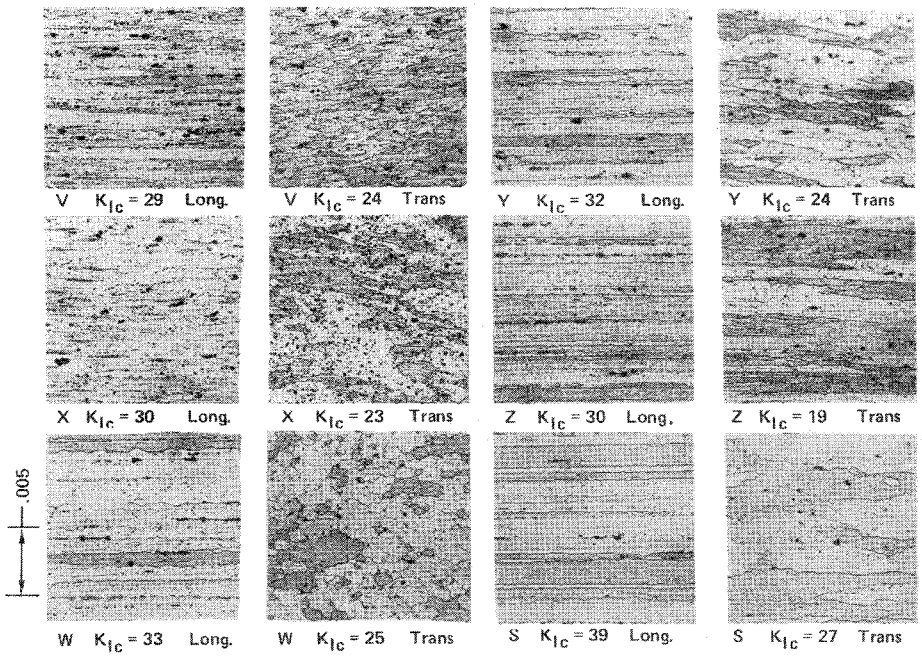

Fig. 13 Typical microstructures of 7075-T76511 (code V) and 7050-T76511 (codes X, W, Y, Z, S) extrusions in the longitudinal (long) and transverse (trans) grain directions.

stress intensities less than K_{Ic}. Stable crack growth continued in some cases, however, in the *LT* specimens after the *TL* specimens had failed. Since the only significant differences in crack growth were in the very high growth rate region, the impact on the design life of a component would be small.

The microstructure of the code S extrusion was significantly "cleaner" than all of the other materials tested, although the chemical analysis data in Table 1 showed comparable iron and silicon contents for all of the 7050-T76511 extrusions. The microstructures are compared in Fig. 13. The code S extrusion also showed the highest fracture toughness values of all of the extrusions tested. Close examination of the fatigue crack growth data in Fig. 10, however, revealed that this extrusion showed crack growth rates generally higher than the others at the higher stress intensities (10–25 ksi$\sqrt{\text{in}}$.

VI. Summary and Conclusions

In view of these findings, it appears that the higher toughness orientations in these materials will offer little or no advantage in corrosive environments but may provide some advantage in very dry air, but only in the higher stress intensity ranges, i.e., approaching $(1-R)(K_{Ic})$. Within the scope of this test, i.e., the materials, composition ranges, measured properties, (especially fracture toughness), etc., the findings indicate that the life prediction analyst should not assume that cleaner, tougher aluminum alloys, or the "redirecting" of load paths into higher toughness "directions" neccesarily will provide improved crack growth rate behavior in corrosive environments.

Fatigue crack growth rates are comparable for the 7050-T76511 and 7075-T76511 extrusion alloys. The crack growth rates did not improve with toughness; however, higher toughness materials or specimen orientations permitted crack growth to longer crack length prior to fracture. Note, however, that this occurs at crack growth rates greater than 100 μin./cycle, thus having only a minor effect on the life of the specimen or part. The 7050-T76511 alloy extrusion provides a significant strength advantage over the 7075-T76511 alloy extrusion and improved stress corrosion resistance over the 7075-T6511 extrusion; however, it is not as strong as the 7075-T6511 material.

References

[1] Staley, J. T., "Investigation to Improve the Stress Corrosion Resistance of Aluminum Aircraft Alloys Through Alloy Additions and Specialized Heat Treatment," Naval Air Systems Command, Contract N00019-68-C-0146, Final Rep. Feb., 1969.

[2] Staley, J. T., "Investigation to Develop a High Strength Stress-Corrosion Resistant Aluminum Aircraft Alloy," Naval Air Systems Command Contract N00019-69-C-0292, Final Rep. Jan., 1970.

[3] Staley, J.T., "Development of a High Strength Stress-Corrosion Resistant Naval Aircraft Alloy," Naval Air Systems Command Contract N00019-70-C-0118, Final Rep. Nov., 1970.

[4] Staley, J. T., and Hunsicker, H. Y., "Exploratory Development of High Strength Stress-Corrosion Resistant Aluminum Alloys Usable in Thick Section Applications," Air Force Materials Lab. Contract F33615-69-C-1644, Phase I, TR AFML-TR-70-256, Nov., 1970.

[5] Staley, J. T., Hunsicker, H. Y., and Schmidt, R., "New Aluminum Alloy X7050," *ASM Metals Congress,* Detroit, Mich., Oct., 1971.

[6] Staley, J. T., "Further Development of Aluminum Alloy X7050," Naval Air Systems Command Contract N00019-71-C-0131, Final Rep., May 8, 1972.

[7] Davies, R. E., Nordmark, G. E., and Walsh, J. D., "Design Mechanical Properties, Fracture Toughness, Fatigue Properties, Exfoliation and Stress Corrosion Resistance of 7050 Sheet, Plate, Extrusions, Hand Forgings and Die Forgings," Naval Air Systems Command Contract N00019-72-0512, July 1975.

[8] Pettit, D. E., Ryder, J. T., Krupp, W. E., and Hoeppner, D. W., "Investigation of the Effects of Stress and Chemical Environment on the Prediction of Fracture in Aircraft Structural Materials," AFML-TR-74-183, Dec. 1974.

[9] Clark, W. G. and Hudak, S. J., "Variability in Fatigue Crack Growth Rate Testing," ASTM E-24.04.01 Task Group Rep., Westinghouse Research Lab. Scientific Paper 74-1E7-MSLRA-P2, Pittsburgh, Pa., Sept. 1974.